

1 **Title:** Detecting neuroendocrine prostate cancer through tissue-informed cell-free DNA  
2 methylation analysis

3  
4 **Authors:** Jacob E. Berchuck<sup>1,2\*</sup>, Sylvan C. Baca<sup>1,2\*</sup>, Heather M. McClure<sup>1,2\*</sup>, Keegan  
5 Korthauer<sup>3,4</sup>, Harrison K. Tsai<sup>5</sup>, Pier Vitale Nuzzo<sup>1,2</sup>, Kaitlin M. Kelleher<sup>1</sup>, Monica He<sup>1</sup>, John A.  
6 Steinharter<sup>1</sup>, Soumya Zacharia<sup>1,2</sup>, Sandor Spisak<sup>1,2</sup>, Ji-Heui Seo<sup>1,2</sup>, Vincenza Conteduca<sup>6</sup>, Olivier  
7 Elemento<sup>7</sup>, Joonghoon Auh<sup>7</sup>, Michael Sigouros<sup>7</sup>, Eva Corey<sup>8</sup>, Michelle S. Hirsch<sup>5</sup>, Mary-Ellen  
8 Taplin<sup>1</sup>, Toni K. Choueiri<sup>1</sup>, Mark M. Pomerantz<sup>1,2</sup>, Himisha Beltran<sup>1</sup>, Matthew L. Freedman<sup>1,2</sup>

9  
10 \* Equal contribution (J.E.B., S.C.B., H.M.M.)

11  
12 **Affiliations:**

13 <sup>1</sup> Department of Medical Oncology, Dana-Farber Cancer Institute, Harvard Medical School;  
14 Boston, Massachusetts, USA

15 <sup>2</sup> Center for Functional Cancer Epigenetics, Dana-Farber Cancer Institute; Boston,  
16 Massachusetts, USA

17 <sup>3</sup> Department of Statistics, University of British Columbia; Vancouver, British Columbia,  
18 Canada

19 <sup>4</sup> BC Children's Hospital Research Institute; Vancouver, British Columbia, Canada

20 <sup>5</sup> Department of Pathology, Brigham and Women's Hospital and Harvard Medical School;  
21 Boston, Massachusetts, USA

22 <sup>6</sup> Unit of Medical Oncology and Biomolecular Therapy, Department of Medical and Surgical  
23 Sciences, University of Foggia; Foggia, Italy

24 <sup>7</sup> Englander Institute for Precision Medicine, Weill Cornell Medicine, New York, New York,  
25 USA

26 <sup>8</sup> Department of Urology, University of Washington; Seattle, Washington, USA

27

28 **Running Title:** NEPC detection using cfDNA

29

30 **Corresponding Author:** Matthew L. Freedman, MD; 450 Brookline Ave, Smith 1058, Boston,  
31 MA, 02215; Phone: 617-582-8598; Fax: 617-632-2165; [mfreedman@partners.org](mailto:mfreedman@partners.org)

32

33 **Conflict of Interest Statement:** JEB, SCB, and MLF are listed as inventors on patents filed that  
34 pertain to the data presented in this manuscript. All other author disclosures are outside the scope  
35 of the current manuscript.

36

37 **Key Words:** Prostate cancer; Metastatic Castration-Resistant Prostate Cancer; Neuroendocrine  
38 Prostate Cancer; Biomarkers; DNA Methylation; Epigenetics

39 **ABSTRACT**

40

41 **Purpose:** Neuroendocrine prostate cancer (NEPC) is a resistance phenotype that emerges in men  
42 with metastatic castration-resistant prostate adenocarcinoma (CR-PRAD) and has important  
43 clinical implications, but is challenging to detect in practice. Herein, we report a novel tissue-  
44 informed epigenetic approach to non-invasively detect NEPC.

45

46 **Experimental Design:** We first performed methylated immunoprecipitation and high-throughput  
47 sequencing (MeDIP-seq) on a training set of tumors, identified differentially methylated regions  
48 between NEPC and CR-PRAD, and built a model to predict the presence of NEPC (termed  
49 NEPC Risk Score). We then performed MeDIP-seq on cell-free DNA (cfDNA) from two  
50 independent cohorts of men with NEPC or CR-PRAD and assessed the accuracy of the model to  
51 predict the presence NEPC.

52

53 **Results:** The test cohort comprised cfDNA samples from 48 men, 9 with NEPC and 39 with CR-  
54 PRAD. NEPC Risk Scores were significantly higher in men with NEPC than CR-PRAD  
55 ( $P=4.3 \times 10^{-7}$ ) and discriminated between NEPC and CR-PRAD with high accuracy (AUROC  
56 0.96). The optimal NEPC Risk Score cut-off demonstrated 100% sensitivity and 90% specificity  
57 for detecting NEPC. The independent, multi-institutional validation cohort included cfDNA from  
58 53 men, including 12 with NEPC and 41 with CR-PRAD. NEPC Risk Scores were significantly  
59 higher in men with NEPC than CR-PRAD ( $P=7.5 \times 10^{-12}$ ) and perfectly discriminated NEPC from  
60 CR-PRAD (AUROC 1.0). Applying the pre-defined NEPC Risk Score cut-off to the validation  
61 cohort resulted in 100% sensitivity and 95% specificity for detecting NEPC.

62

63 **Conclusions:** Tissue-informed cfDNA methylation analysis is a promising approach for non-  
64 invasive detection of NEPC in men with advanced prostate cancer.

65

## 66 **STATEMENT OF TRANSLATIONAL RELEVANCE**

67

68 Early detection of neuroendocrine prostate (NEPC) is challenging in clinical practice, but has  
69 important prognostic and therapeutic implications for men with metastatic castration-resistant  
70 prostate cancer (mCRPC). In the largest study to date of cell-free DNA (cfDNA) from men with  
71 NEPC, we developed and validated a non-invasive NEPC Risk Score using tissue-informed  
72 cfDNA methylation analysis. Applying the NEPC Risk Score to cfDNA from two independent  
73 cohorts of men with mCRPC resulted in highly accurate discrimination between men with versus  
74 without NEPC. In both cohorts, high NEPC Risk Score was associated with significantly worse  
75 overall survival. These data strongly support the clinical utility of this cfDNA methylation-based  
76 NEPC Risk Score in men with mCRPC to non-invasively identify those who should be  
77 considered for platinum-based chemotherapy or clinical trials of novel NEPC-directed therapies.

78

## 79 **INTRODUCTION**

80

81 Neuroendocrine prostate cancer (NEPC) can arise as a resistance mechanism to androgen  
82 deprivation therapy (ADT) and androgen receptor signaling inhibitors (ARSIs) in men with  
83 metastatic castration-resistant prostate cancer (mCRPC).(1,2) Present in up to 17% of men with  
84 mCRPC, NEPC is associated with poor response to ARSIs and shorter overall survival

85 (OS).(1,3) However, NEPC tumors are more likely to respond to platinum-based chemotherapy  
86 and several novel NEPC-directed therapies are in clinical development.(4)

87

88 The current approach to diagnosing NEPC – performing tissue biopsy for pathologic tumor  
89 analysis – has significant shortcomings. There is a lack of consensus pathological criteria for  
90 defining NEPC and, due to intra-patient tumor heterogeneity, biopsy samples may not represent  
91 a patient’s overall disease burden.(5–7) Consequently, NEPC diagnosis is often delayed or  
92 missed and reported rates likely underestimate the prevalence of this aggressive disease variant.  
93 The lack of a biomarker for early and accurate detection is a significant barrier to improving  
94 outcomes for men who develop NEPC.

95

96 Liquid biopsies are well-suited to address this unmet need. Most clinical cell-free DNA (cfDNA)  
97 tests detect somatically acquired tumor mutations or copy number alterations. However, the  
98 defining genetic hallmark of NEPC, deleterious alterations in *RBI* and/or *TP53*, are present in  
99 more than one-third of castration-resistant prostate adenocarcinoma (CR-PRAD) tumors and thus  
100 cannot unambiguously discriminate between the tumor subtypes.(1) In contrast, vast DNA  
101 methylation differences exist between NEPC and CR-PRAD.(5) Cell-free methylated DNA  
102 immunoprecipitation and high-throughput sequencing (cfMeDIP-seq), a highly sensitive method  
103 for genome-wide cfDNA methylation profiling, capable of non-invasive cancer detection and  
104 discriminating between tumor types, is well-suited to non-invasively detect NEPC.(8–10)

105

106 In this manuscript, we evaluate the ability of cfMeDIP-seq to detect NEPC in men with mCRPC.  
107 We first perform methylation profiling on a training set of NEPC and PRAD tumors to identify

108 methylation sites enriched in each tumor type. We then establish the ability to implement tissue-  
109 informed analysis of cfMeDIP-seq data to detect NEPC in cfDNA from men with NEPC or CR-  
110 PRAD. Finally, in an independent cfDNA cohort from men with NEPC or CR-PRAD, we  
111 confirm the analytical and clinical validity of this approach for accurate, non-invasive detection  
112 of NEPC.

113

## 114 **MATERIALS AND METHODS**

115

### 116 **Subjects and samples**

117

118 Plasma samples were collected from men with mCRPC diagnosed and treated at the Dana-Farber  
119 Cancer Institute (DFCI), Brigham and Women's Hospital, or Weill Cornell Medicine (WCM)  
120 between April 2003 and August 2021. Two genitourinary pathologists (H.K.T. and M.S.H.)  
121 confirmed the presence of high-grade neuroendocrine carcinoma of prostate origin according to  
122 modern conventions based on histologic review of available material, re-interpretation of original  
123 reports, and integration of available molecular results.(11) CR-PRAD patients had castration-  
124 resistant prostate adenocarcinoma with no pathologic evidence of neuroendocrine differentiation  
125 throughout their disease course. All patients provided written informed consent. The use of  
126 samples was approved by the DFCI (01-045 and 09-171) and WCM (1305013903). Studies were  
127 conducted in accordance with recognized ethical guidelines. The previously-described LuCaP  
128 PDXs were derived from resected metastatic prostate cancer with informed consent of patient  
129 donors under a protocol approved by the University of Washington Human Subjects Division  
130 IRB.(12)

131

132 **Sample processing**

133

134 cfDNA samples were processed by the following method. Peripheral blood was collected in  
135 EDTA Vacutainer tubes (BD), and processed within 3 hours of collection. Plasma was separated  
136 by centrifugation at 2,500 g for 10 minutes, transferred to microcentrifuge tubes, and centrifuged  
137 at 2,500 g at room temperature for 10 minutes to remove cellular debris. The supernatant was  
138 aliquoted into 1-2 mL aliquots and stored at -80°C until the time of DNA extraction. cfDNA was  
139 isolated from 1 mL of plasma, using the Qiagen Circulating Nucleic Acids Kit (Qiagen), eluted  
140 in AE buffer, and stored at -80°C. DNA from the LuCaP PDXs was extracted using the DNeasy  
141 Blood and Tissue Kit (Qiagen). Genomic DNA was sheared using a Covaris Sonicator E220 and  
142 AMPure XP beads (Beckman Coulter) were used to size select 150-250 bp DNA fragments.

143

144 **cfDNA tumor content calculation**

145

146 Low-pass whole genome sequencing (LPWGS) was performed on all cfDNA samples. The  
147 ichorCNA R package was used to infer copy number profiles and cfDNA tumor content from  
148 read abundance across bins spanning the genome using default parameters.(13)

149

150 **cfMeDIP-seq protocol**

151

152 cfMeDIP-seq was performed using previously published methods.(10) cfDNA library  
153 preparation was performed using KAPA HyperPrep Kit (KAPA Biosystems) according to the

154 manufacturer's protocol. We then performed end-repair, A-tailing, and ligation of NEBNext  
155 adaptors (NEBNext Multiplex Oligos for Illumina kit, New England BioLabs). Libraries were  
156 digested using the USER enzyme (New England BioLabs).  $\lambda$  DNA, consisting of unmethylated  
157 and *in vitro* methylated DNA, was added to prepared libraries to achieve a total amount of 100  
158 ng DNA. Methylated and unmethylated *Arabidopsis thaliana* DNA (Diagenode) was added for  
159 quality control. MeDIP was performed using the MagMeDIP kit (Diagenode) following the  
160 manufacturer's protocol. Samples were purified using the iPure Kit v2 (Diagenode). Success of  
161 the immunoprecipitation was confirmed using qPCR to detect recovery of the spiked-in  
162 *Arabidopsis thaliana* methylated and unmethylated DNA.

163

#### 164 **Next-generation sequencing library construction**

165

166 KAPA HiFi Hotstart ReadyMix (KAPA Biosystems) and NEBNext Multiplex Oligos for  
167 Illumina (New England Biolabs) were added to a final concentration of 0.3  $\mu$ M and libraries  
168 were amplified as follows: activation at 95°C for 3 minutes, amplification cycles of 98°C for 20  
169 seconds, 65°C for 15 seconds, 72°C for 30 seconds, and a final extension of 72°C for 1 minute.  
170 Samples were pooled and sequenced (Novogene Corporation, CA) on Illumina HiSeq 4000 to  
171 generate 150 bp paired-end reads.

172

#### 173 **Quality control and processing of sequencing reads**

174

175 After sequencing, the quality and quantity of the raw reads were examined using FastQC version  
176 0.11.5 (<http://www.bioinformatics.babraham.ac.uk/projects/fastqc>) and MultiQC version 1.7.(14)



177 Raw reads were quality and adapter trimmed using Trim Galore! version 0.6.0  
178 ([http://www.bioinformatics.babraham.ac.uk/projects/trim\\_galore/](http://www.bioinformatics.babraham.ac.uk/projects/trim_galore/)) using default settings in  
179 paired-end mode. The trimmed reads then were aligned to hg19 using Bowtie2 version 2.3.5.1 in  
180 paired-end mode and all other settings default.(15) The SAMtools version 1.10 software suite  
181 was used to convert SAM alignment files to BAM format, sort and index reads, and remove  
182 duplicates.(16) The R package RSamtools version 2.2.1 was used to calculate the number of  
183 unique mapped reads. Saturation analyses to evaluate reproducibility of each library were carried  
184 out using the R Bioconductor package MEDIPS version 1.38.0.(17)

185

### 186 **Tissue-informed approach to NEPC detection**

187

188 To identify DMRs between NEPC and PRAD tumors, we first binned the genome into 300 base-  
189 pair windows and tested each window for differential methylation between NEPC and PRAD  
190 samples using limma-voom (using R package limma version 3.42.0) on TMM-normalized counts  
191 (using R package edgeR version 3.28.0).(18,19) Only bins with a total count above a fixed  
192 threshold were tested for differential methylation, where the threshold was set at 20% of the total  
193 number of samples across both groups. We restricted our search to bins within annotated CpG  
194 islands and FANTOM5 enhancers and excluded regions of high signal or poor  
195 mappability.(20,21) We selected DMRs with read enrichment in NEPC compared to PRAD  
196 PDXs at FDR-adjusted  $P < 1.0 \times 10^{-6}$  and  $\log_2$  fold-change  $> 3$ . We removed windows with peaks in  
197 MeDIP-seq data from white blood cells (as determined by MACS2, version 2.1.2) to minimize  
198 signal from blood cell-derived cfDNA.(22) Using the MeDIPs R package, we calculated a CpG-  
199 normalized relative methylation scores across 300 bp windows for each cfDNA sample.(17,23)

200 We then summed relative methylation scores in cfDNA at NEPC-enriched PDX DMRs for each  
201 sample and normalized this value to the sum of rms values across all 300bp windows. This value  
202 was termed “NEPC Methylation Value.” The same process was performed for PRAD-enriched  
203 PDX DMRs to derive a “PRAD Methylation Value.” We then calculated the  $\log_2$  ratio of the  
204 NEPC Methylation Value to the PRAD Methylation Value and normalized these values to the  
205 median score in cfDNA from eight healthy cancer-free controls. This value was termed the  
206 “NEPC Risk Score.” This approach is summarized in Fig. 1A.

207

### 208 **Statistical analysis**

209

210 Comparisons between two groups were calculated using a Wilcoxon rank-sum test. To determine  
211 the accuracy of the NEPC Risk Score for discriminating between cfDNA samples from men with  
212 NEPC versus CR-PRAD, the AUROC was calculated using JMP version 16. The optimal cut-off  
213 for classifying NEPC versus CR-PRAD samples based on NEPC Risk Scores in the cfDNA test  
214 cohort was calculated using Youden’s index ( $J = \text{sensitivity} + \text{specificity} - 1$ ). The optimal cut-  
215 off was determined as the point with the maximum index value. OS was defined as time from  
216 radiographic evidence of metastatic disease to death. Living patients were censored at the last  
217 evaluation. OS was estimated using the Kaplan-Meier method. P-values were calculated using  
218 log-rank test. All P-values were two-sided.

219

### 220 **Data and materials availability**

221

222 The cfMeDIP-seq NGS data for patient samples that support the findings of this study are  
223 available upon request from the corresponding author (M.L.F.) to comply with the DFCI ethics  
224 regulations to protect patient privacy. All requests for raw and analyzed data will be promptly  
225 reviewed by the Belfer Office for Dana-Farber Innovations to verify if the request is subject to  
226 any intellectual property or confidentiality obligations. Any data and materials that can be shared  
227 will be released via a Data Transfer Agreement. All code used to process the data and carry out  
228 the analyses described in the methods is in a publicly available GitHub repository at:  
229 <https://github.com/scbaca/cfmedip>.

230

## 231 **RESULTS**

232

### 233 **Identification of NEPC- and PRAD-enriched DMRs in a tumor training set**

234

235 Prior applications of cfMeDIP-seq for non-invasive cancer detection identified DMRs directly in  
236 cfDNA between highly disparate patient groups, such as cancer versus no cancer.(8–10)  
237 However, as men with mCRPC who develop NEPC often have concurrent PRAD, this limits the  
238 ability to identify NEPC-specific DMRs directly in cfDNA. To address this unique challenge, we  
239 developed a novel tissue-informed strategy for analyzing cfMeDIP-seq data (Fig. 1A). We first  
240 performed MeDIP-seq on 29 LuCaP PDXs, including 5 NEPC and 24 PRAD tumors  
241 (Supplementary Table S1).(12) We chose to analyze PDXs based on recent single-cell analyses  
242 of mCRPC clinical biopsy specimens, which revealed significant intra-tumoral heterogeneity,  
243 including admixed NEPC and PRAD cell populations.(24,25) In contrast, the LuCaP PDXs,

244 which have undergone comprehensive pathologic and molecular characterization, provide a more  
245 pure source of NEPC and PRAD tumor cells.(12)

246

247 Differential methylation analysis of the LuCaP PDXs identified 39,699 NEPC-enriched and  
248 137,692 PRAD-enriched DMRs (FDR-adjusted  $P < 0.05$ ) (Fig. 1B).(12) To ensure that the PDX  
249 methylation data is representative of clinical biopsy specimens, we compared the LuCaP-derived  
250 NEPC- and PRAD-enriched DMRs to DNA methylation data generated from an independent set  
251 of castration-resistant NEPC and PRAD tumors using reduced-representation bisulfite  
252 sequencing.(5) We observed a high correlation between NEPC- and PRAD-enriched DMRs from  
253 the LuCaP PDXs and the clinical biopsy specimens ( $\rho = 0.73$ ;  $P < 2.2 \times 10^{-16}$ ) (Fig. 1C).

254

255 We then identified a subset of NEPC- and PRAD-enriched DMRs that could be used to non-  
256 invasively detect NEPC. Using a stringent cut-off of FDR-adjusted  $P < 1.0 \times 10^{-6}$  and  $\log_2$  fold-  
257 change  $> 3$ , we identified 432 NEPC-enriched and 1,086 PRAD-enriched DMRs. As the majority  
258 of cfDNA is derived from leukocytes, we removed sites that were methylated in WBCs from  
259 age-matched male controls (N=1,165), resulting in a final set of 76 NEPC-enriched and 277  
260 PRAD-enriched DMRs. The *SPDEF* gene highlights the importance of this step. While *SPDEF*  
261 was methylated in NEPC and unmethylated in PRAD tumors, it is also methylated in WBCs  
262 (Fig. 1D). The inability to determine whether a methylated cfDNA fragment at this locus  
263 originated from NEPC or WBCs renders it uninformative for detecting NEPC and could  
264 contribute to misclassification. As exemplified in *UNC13A*, a gene associated with neural  
265 signaling, the final set of DMRs are methylated in one tumor type and unmethylated in the

266 opposite tumor type and WBCs. Consequently, cfDNA fragments at these loci indicate the  
267 presence of NEPC or PRAD.

268

269 To ensure that the final set of tumor-derived DMRs retained biological relevance, we assessed  
270 nearby genes for Gene Ontology (GO) term enrichment.(26) The top GO terms in NEPC-  
271 enriched DMRs pertained to neural development and differentiation, whereas PRAD-enriched  
272 DMRs related to hormone signaling and epithelial cell differentiation, suggesting that the final  
273 set of tumor-derived DMRs reflect the divergent gene regulatory programs of NEPC and PRAD  
274 (Fig. 1E).

275

#### 276 **Classification of NEPC and CR-PRAD samples in a cfDNA test cohort**

277

278 To evaluate the ability to accurately detect NEPC using the novel tissue-informed approach, we  
279 analyzed a test cohort of plasma cfDNA samples from 56 men with mCRPC, including 11 with  
280 NEPC and 45 with CR-PRAD. We first performed LPWGS on all cfDNA samples and  
281 calculated tumor content using ichorCNA, an analytical tool that estimates cfDNA tumor  
282 fraction based on somatic copy number alterations.(13) Based on the ichorCNA lower limit of  
283 detection (3% tumor fraction), 48 (86%) of the 57 cfDNA samples had detectable tumor DNA  
284 including 9 (82%) and 39 (87%) of NEPC and CR-PRAD patients, respectively.(13) cfDNA  
285 samples with less than 3% tumor content were excluded from methylation analysis  
286 (Supplementary Fig. S1). These results compare favorably to a published cfDNA analysis of 269  
287 samples from men with metastatic prostate cancer that detected tumor DNA in 83% of samples  
288 using LPWGS and hybrid-capture targeted sequencing.(27)

289  
290 Characteristics of men in the cfDNA test cohort at the time of plasma collection are listed in  
291 Table 1. Consistent with known decoupling of prostate specific antigen (PSA) from its typical  
292 association with disease burden in NEPC, the median PSA was 0.37 for NEPC patients (range  
293 0.03-3.7) and 140 for CR-PRAD patients (range 0.79-4305).(11) Median cfDNA tumor content  
294 was 15% for men with NEPC (range 5.1-75%) and 21% for those with CR-PRAD (range 3.3-  
295 80%) (P=0.89) (Table 1; Supplementary Fig. S2A).

296  
297 To evaluate to the ability to detect NEPC in cfDNA from men with mCRPC, we first performed  
298 cfMeDIP-seq on the test cohort samples. We then derived an NEPC Methylation Value and  
299 PRAD Methylation Value for each sample by summing the methylated cfDNA fragments at  
300 tissue-derived NEPC-enriched and PRAD-enriched DMRs, respectively (Fig. 1A). An NEPC  
301 Risk Score was calculated for each sample as the normalized ratio of the NEPC Methylation  
302 Value versus the PRAD Methylation Value.

303  
304 We observed significantly higher NEPC Methylation Values in men with NEPC than CR-PRAD  
305 (median  $8.1 \times 10^{-6}$  versus  $6.3 \times 10^{-6}$ ; P=0.0025) (Fig. 2A). In contrast, PRAD Methylation Values  
306 were significantly higher in men with CR-PRAD than NEPC (median  $5.4 \times 10^{-5}$  versus  $4.1 \times 10^{-5}$ ;  
307 P= $4.3 \times 10^{-6}$ ) (Fig. 2B). NEPC Risk Scores were significantly higher in men with NEPC than  
308 those with CR-PRAD (median 0.35 versus -0.14; P= $4.3 \times 10^{-7}$ ) (Fig. 2C). The AUROC for  
309 accurate classification of men with NEPC versus CR-PRAD based on NEPC Risk Score was  
310 0.96. The optimal NEPC Risk Score cut-off (high  $>0.15$  versus low  $\leq 0.15$ ) demonstrated 100%  
311 sensitivity and 90% specificity for detecting NEPC. Further, high versus low NEPC Risk Score

312 was associated with significantly shorter OS from the time of metastatic prostate cancer (hazard  
313 ratio [HR]=2.5; 95% confidence interval [95%CI]=1.2-4.8; P=0.017) (Fig. 2D). Median OS was  
314 32 months shorter for men with high (14 months) versus low (46 months) NEPC Risk Scores.

315

### 316 **Classification of NEPC and CR-PRAD samples in an independent cfDNA validation cohort**

317

318 To assess the reproducibility of this approach and the NEPC Risk Score cut-off, we identified an  
319 independent multi-institutional validation cohort of plasma samples from 73 men with mCRPC  
320 at DFCI and WCM, including 16 men with NEPC and 57 with CR-PRAD. cfDNA LPWGS  
321 identified tumor DNA in 53 (73%) of samples including 12 (75%) and 48 (72%) of NEPC and  
322 CR-PRAD patients, respectively. cfDNA samples with less than 3% tumor content were  
323 excluded from methylation analysis (Supplementary Fig. S1). Median cfDNA tumor content was  
324 23% for NEPC patients (range 3.4-43%) and 16% for CR-PRAD patients (range 3.8-39%) in the  
325 test cohort (P=0.49) (Supplementary Fig. S2B; Table 1). Median PSA was 0.33 (range 0.01-6.23)  
326 in men with NEPC versus 112 (range 4.5-1821) in those with CR-PRAD. Differences between  
327 men with NEPC and CR-PRAD in the cfDNA validation cohort were similar to those observed  
328 in the cfDNA test cohort (Table 1).

329

330 As we observed in the test cohort, NEPC samples in the cfDNA validation cohort exhibited  
331 significantly higher NEPC Methylation Values (median  $9.6 \times 10^{-6}$  versus  $6.4 \times 10^{-6}$ ;  $P=1.5 \times 10^{-4}$ ),  
332 lower PRAD Methylation Values (median  $4.5 \times 10^{-5}$  versus  $5.5 \times 10^{-5}$ ;  $P=0.0013$ ), and higher  
333 NEPC Risk Scores (median 0.69 versus -0.19;  $P=7.5 \times 10^{-12}$ ) than those with CR-PRAD (Figs.  
334 3A-C). The AUROC for accurate classification of men with NEPC versus CR-PRAD based on

335 NEPC Risk Score was 1.0. Applying the NEPC Risk Score cut-off derived in the test cohort  
336 (high  $>0.15$  versus low  $\leq 0.15$ ) to the cfDNA validation cohort resulted in 100% sensitivity and  
337 95% specificity for detecting NEPC. High versus low NEPC Risk Score was associated with  
338 significantly shorter OS from the time of metastatic prostate cancer (HR=4.3, 95% CI=2.9-8.9;  
339  $P=3.2 \times 10^{-4}$ ) (Fig. 3D). Median OS was 36 months shorter for men with high (20 months) versus  
340 low (56 months) NEPC Risk Scores. Notably, there was no association of cfDNA tumor content  
341 with OS across the two cfDNA cohorts (Supplementary Fig. S3), suggesting that the negative  
342 correlation between NEPC Risk Score and OS is driven by different tumor biology and not  
343 higher disease burden.

344

#### 345 **Patient vignettes highlight NEPC risk factors in misclassified CR-PRAD samples**

346

347 To understand potential factors driving misclassification, we reviewed medical histories for the  
348 six patients with CR-PRAD with NEPC Risk Scores  $>0.15$  across the two cfDNA cohorts. Five  
349 of these patients had clinical, radiographic, and genomic features associated with NEPC (Fig. 4).  
350 The two patients with the highest NEPC Risk Score (0.50 and 0.36) both previously received  
351 abiraterone, docetaxel, cabazitaxel, and were on enzalutamide at the time of cfDNA collection.  
352 The first patient's CT scan six days after cfDNA collection showed marked increase in  
353 metastatic tumor burden, including new liver metastases. He subsequently experienced clinical  
354 deterioration and died five weeks later. The second patient previously underwent somatic tumor  
355 profiling revealing two-copy *RBI* deletion. He experienced clinical deterioration and died 8  
356 weeks after cfDNA collection. The next three patients had all received prior abiraterone and/or  
357 enzalutamide. The first (NEPC Risk Score of 0.27) was progressing on abiraterone and



358 underwent tumor biopsy at the time of cfDNA collection showing poorly differentiated  
359 carcinoma harboring single-copy *RBI* loss and two deleterious *TP53* alterations. The second  
360 patient (NEPC Risk Score of 0.24) previously received abiraterone and was progressing on  
361 enzalutamide at the time of cfDNA collection. Genomic profiling two months earlier showed that  
362 the patient's tumor harbored biallelic loss of *RBI* and *TP53*. The third patient (NEPC Risk Score  
363 of 0.20) previously received abiraterone and at the time of cfDNA collection was progressing on  
364 docetaxel with CT scan showing new liver metastases. He experienced clinical deterioration and  
365 died two months later. These hypothesis-generating vignettes suggest the possibility that the  
366 cfDNA NEPC Risk Score may identify occult NEPC not detected through routine clinical care.  
367

#### 368 **Association of the plasma cfDNA methylome with NEPC Risk Score and tumor content**

369  
370 Prior data suggest that the plasma cfDNA methylome strongly correlates with tumor content in  
371 men with metastatic prostate cancer.(28) As such, we sought to understand the association of the  
372 cfDNA methylome in this cohort with tumor content. We first performed principal component  
373 analysis (PCA) of the genome-wide methylome data (Fig. 5A) and the methylation data at the  
374 NEPC- and PRAD-enriched DMRs included in the NEPC Risk Score (Fig. 5B) for the 101  
375 cfDNA samples included in the NEPC Risk Score analyses. In the genome-wide data, the first  
376 principal component (PC1) is driven by an outlier sample with high CpG enrichment relative to  
377 the others. There was otherwise no separation of NEPC and CR-PRAD samples in PC1 and PC2  
378 in the genome-wide methylome data (Fig. 5A). However, at the DMR sites, PC1 and PC2 clearly  
379 separated NEPC and CR-PRAD samples (Fig. 5B).  
380

381 We next quantified the correlation between each of the first 10 PCs with NEPC Risk Score and  
382 cfDNA tumor content. For the genome-wide data, not until PC8, which explained 2.2% of  
383 variance, was there a robust correlation with NEPC Risk Score ( $R^2=0.32$ ;  $P=7.3 \times 10^{-10}$ ) (Fig. 5C;  
384 Supplementary Fig. S4A). In contrast, when limiting to the DMRs included in the NEPC Risk  
385 Score, PC1 ( $R^2=0.34$ ;  $P=1.2 \times 10^{-10}$ ), which explained 30% of variance, and PC2 ( $R^2=0.42$ ;  
386  $P=2.0 \times 10^{-13}$ ), which explained 8.3% of variance, both demonstrated robust correlation with  
387 NEPC Risk Score (Fig. 5D; Supplementary Fig. S4B). We then quantified the correlation  
388 between the top PCs and cfDNA tumor content. In the genome-wide methylome data, PC2,  
389 which explained 4.2% of variance, correlated with cfDNA tumor content ( $R^2=0.34$ ;  $P=1.7 \times 10^{-10}$ )  
390 (Fig. 5E; Supplementary Fig. S4A). This result affirms the prior finding that the prostate cancer  
391 plasma cfDNA methylome correlates with cfDNA tumor content.(28) When limiting to the  
392 DMRs included in the NEPC Risk Score, PC1 ( $R^2=0.22$ ;  $P=7.2 \times 10^{-7}$ ) and PC2 ( $R^2=0.29$ ;  
393  $P=5.1 \times 10^{-9}$ ) correlated with cfDNA tumor content, though not to the same extent they correlated  
394 with NEPC Risk Score (Fig. 5F; Supplementary Fig. S4B).

395  
396 Finally, we assessed the correlation between NEPC Risk Score and cfDNA tumor content (Fig.  
397 5G). Across all NEPC and CR-PRAD cfDNA samples, there was no correlation between NEPC  
398 Risk Score and tumor content ( $R^2=0.0033$ ;  $P=0.57$ ); there was also no correlation in the PRAD  
399 samples ( $R^2=0.010$ ;  $P=0.37$ ). NEPC Risk Score and tumor content did significantly correlate in  
400 the cfDNA samples from men with NEPC ( $R^2=0.24$ ;  $P=0.025$ ). Given this association,  
401 suggesting lower NEPC Risk Scores in men with lower cfDNA tumor content, we evaluated the  
402 diagnostic performance of the NEPC Risk Score in the NEPC and CR-PRAD samples across the  
403 two cohorts with cfDNA tumor content less than 10%. The NEPC Risk Score in these patients

404 resulted in an AUROC of 0.93; applying the NEPC Risk Score cut-off of 0.15 resulted in 100%  
405 sensitivity and 82% specificity for detecting NEPC (data not shown).

406

## 407 **DISCUSSION**

408

409 NEPC is an aggressive, clinically actionable resistance phenotype that can emerge in men with  
410 mCRPC. The challenge of identifying NEPC in routine clinical practice leads to delays in  
411 diagnosis and underdiagnosis. In the largest study to date of cfDNA from men with NEPC, we  
412 present a novel approach for tissue-informed analysis of cfMeDIP-seq data, leading to highly  
413 accurate non-invasive detection of NEPC. We first identified methylation sites enriched in a  
414 training set of NEPC and PRAD tumors. Tissue-informed methylation analysis of two  
415 independent cohorts of cfDNA from men with pathologically confirmed NEPC or CR-PRAD,  
416 demonstrated high accuracy (AUROC of 0.96 and 1.0). Importantly, applying a diagnostic cut-  
417 off derived in the cfDNA test cohort to the independent validation cohort resulted in 100%  
418 sensitivity and 95% specificity for detecting NEPC. Finally, in both cfDNA cohorts, a high  
419 NEPC Risk Score was associated with significantly shorter OS (HR of 2.5 and 4.3). This work  
420 strongly supports the analytical and clinical utility of tissue-informed analysis of cfMeDIP-seq  
421 data to non-invasively detect NEPC in men with mCRPC.

422

423 The current approach for diagnosing NEPC has significant shortcomings that could be overcome  
424 with a liquid biopsy. The lack of consensus pathological criteria highlights the advantage of an  
425 objective biomarker. Herein, we demonstrated that tissue-informed analysis of cfMeDIP-seq data  
426 provides a quantitative readout (NEPC Risk Score) that discriminated between men with NEPC

427 or CR-PRAD with high accuracy in two independent cfDNA cohorts. The ability to apply a  
428 diagnostic cut-off from one cfDNA cohort to an independent cohort while maintaining excellent  
429 diagnostic accuracy suggests this quantitative approach is robust and reproducible. An additional  
430 benefit of a liquid biopsy to detect NEPC is that cfDNA may be more representative of a  
431 patient's overall tumor burden than tissue biopsy of a single metastatic focus.(29) Intra-patient  
432 tumor heterogeneity is well-established in mCRPC.(6) This is highly relevant in this clinical  
433 context, as NEPC often emerges as a treatment-resistant subclone and can be missed due to  
434 sampling error with a single tissue biopsy. Future studies analyzing cfDNA from patients  
435 undergoing autopsy or correlating cfDNA results with molecular imaging could provide further  
436 insight into how representative NEPC Risk Scores are of intra-patient NEPC versus PRAD  
437 tumor burden. However, we establish in this report that the NEPC Risk Score is a highly accurate  
438 quantitative non-invasive biomarker that is highly predictive of the presence or absence of NEPC  
439 in men with mCRPC.

440

441 Detecting NEPC has important prognostic implications. Compared to men with CR-PRAD,  
442 NEPC is associated with shorter OS.(1) Consistent with this known negative prognostic  
443 association, we observed that high NEPC Risk Score (relative to the diagnostic cut-off) was  
444 associated with significantly shorter OS in two independent cfDNA cohorts. Aggarwal et al  
445 reported a HR of 1.8 (95%CI=1.0-3.2) for OS in men with versus without treatment-emergent  
446 small-cell neuroendocrine prostate cancer.(1) The HRs for OS in our cohorts were 2.5  
447 (95%CI=1.2-4.8) and 4.3 (95%CI=2.0-8.9). The worse prognosis of men with high NEPC Risk  
448 Score in our study may reflect differences in patient characteristics. We included only men with  
449 morphologic high-grade neuroendocrine carcinoma and not PRAD with expression of

450 neuroendocrine markers by immunohistochemistry – the latter is not as clearly associated with a  
451 virulent clinical course as the former.(11)

452

453 Early and accurate detection of NEPC also has important therapeutic implications. While men  
454 with NEPC are characteristically unresponsive to ARSIs, they are more likely to respond to  
455 platinum-based chemotherapy.(4) Consequently, NCCN guidelines recommend treatment with  
456 platinum chemotherapy combined with etoposide or a taxane.(30) Histology-specific treatment  
457 recommendations highlight the immediate clinical actionability of detecting NEPC. With several  
458 ongoing clinical trials testing novel therapeutic approaches in men with NEPC, the implications  
459 of detecting this disease variant will likely increase in the coming years.(31) While the  
460 association of the NEPC Risk Score with response to prostate cancer therapy remains to be  
461 established, we encourage incorporating cfDNA collection into prospective clinical trials to  
462 facilitate future studies to develop and validate non-invasive biomarkers to identify patients  
463 likely to benefit from NEPC-directed therapy.

464

465 Successful cfDNA-based biomarkers must be accurate, cost-effective, and practical to implement  
466 in clinical practice. Beltran et al previously reported the feasibility of non-invasively detecting  
467 NEPC-specific DNA methylation in cfDNA using whole-genome bisulfite sequencing  
468 (WGBS).(7) However, test characteristics for distinguishing men with NEPC versus CR-PRAD  
469 using this approach were not reported. Compared to WGBS, cfMeDIP-seq has several  
470 advantages. The high cost of whole-genome sequencing currently limits the ability to implement  
471 WGBS in clinical practice. In contrast, by only sequencing methylated cfDNA, cfMeDIP-seq  
472 provides genome-wide methylation data at a fraction of the cost of WGBS. Further, cfMeDIP-

473 seq only requires 5-10 ng of cfDNA, which can be obtained from 1 ml of plasma. While direct  
474 comparison of the performance of these approaches will be informative, the low cost, small  
475 sample requirement, and high sensitivity highlight advantages of cfMeDIP-seq as the basis for a  
476 clinical biomarker.

477

478 The methods presented in this manuscript represent an important advance for developing cfDNA  
479 methylation-based clinical biomarkers. Several recent publications highlight advantages of  
480 epigenetic compared to genetic liquid biopsy approaches.(32–34) Whereas previous studies  
481 performed unsupervised analysis of cfMeDIP-seq data, we developed a novel tissue-informed  
482 method, which benefits from the strength of its biological basis. Tissue-informed analysis  
483 ensures that the model is built upon molecular features known to be present in and specific to the  
484 tumor of interest. This contrasts with the tumor-naïve approach of developing a methylation  
485 signature directly in cfDNA (*e.g.*, from individuals with cancer versus without cancer), which  
486 risks overfitting due to signal unrelated to cancer (*e.g.*, sex, age, smoking status, comorbid  
487 disease, etc). Principal component analysis emphasized the value of this tissue-informed  
488 approach. In the genome-wide cfDNA methylome data, not until PC8, which explained only  
489 2.2% of variance, did we observe a correlation with the methylation signal that distinguished  
490 NEPC from CR-PRAD samples. However, the methylation data at the tissue-derived NEPC- and  
491 PRAD-enriched DMRs revealed a strong correlation between NEPC Risk Score and PCs 1 and  
492 2, which explained nearly 40% of variance. We believe that the methods presented herein will  
493 help facilitate detection of clinically relevant cancer phenotypes. Aberrant DNA methylation is  
494 present across tumor types with several clinically actionable subtypes harboring distinct  
495 methylation profiles, such as *IDH*-mutant gliomas and microsatellite instability (MSI) high

496 uterine and colon cancers.(35–38) As our understanding of clinically-actionable epigenetically-  
497 distinct cancer phenotypes evolves, the methods presented in this manuscript will facilitate non-  
498 invasive detection of these tumor subtypes.

499

500 While our results strongly support the feasibility of using cfMeDIP-seq to non-invasively detect  
501 NEPC in men with mCRPC, it is appropriate to recognize several potential limitations. First, is  
502 the number of patients with NEPC included in the study. The cfDNA test and validation cohorts  
503 contained 21 men with NEPC. While this number is small in absolute terms, it represents the  
504 largest analysis to date of cfDNA from men with pathologically-confirmed NEPC. While  
505 similarly high accuracy was observed across two independent cfDNA cohorts, the reproducibility  
506 and clinical validity will benefit from further prospective validation. It is also important to  
507 acknowledge that this was a retrospective and heterogeneous cohort, which introduces potential  
508 confounding factors, mainly patient selection. This limits our ability to conclusively establish  
509 that NEPC Risk Score is associated with inferior clinical outcomes. However, that the NEPC  
510 Risk Score performs so well despite the heterogeneity in the cohort speaks to the robustness of  
511 the methylation signal and the ability of the assay and methods to detect it. Another limitation is  
512 that NEPC patients in this study were limited to men with high-grade neuroendocrine carcinoma  
513 and did not include those with PRAD with neuroendocrine differentiation.(11) Thus, we cannot  
514 comment on whether the NEPC Risk Score discriminates between these two variants. Likewise,  
515 all men in the NEPC group had biopsy-proven high-grade neuroendocrine carcinoma at the time  
516 of plasma collection. We did not evaluate plasma samples in men prior to NEPC diagnosis when  
517 the relative abundance of NEPC-derived cfDNA may be lower and thus harder to detect. As  
518 such, we were not able to establish how early in the disease course this biomarker can detect

519 treatment-emergent NEPC. Finally, as we limited the methylation analysis to men with  
520 detectable circulating tumor DNA by ichorCNA, we did not assess how the assay performs in  
521 men with very low cfDNA tumor content. More work is needed to fully establish the relationship  
522 between NEPC Risk Score with cfDNA tumor content. Several additional questions remain:  
523 What is the analytical limit of detection of this cfDNA methylation-based approach for detecting  
524 NEPC? What is the optimal timing to evaluate cfDNA in men with mCRPC to identify NEPC?  
525 How long before clinical diagnosis can NEPC be detected in cfDNA? Will early detection and  
526 initiation of platinum-based chemotherapy improve clinical outcomes for men diagnosed with  
527 NEPC? We hope to address these questions in future studies.

528

529 In summary, we demonstrated the analytical and clinical utility of tissue-informed cfDNA  
530 methylation analysis to non-invasively detect NEPC in men with mCRPC. These findings  
531 support further studies to establish the prognostic and predictive value of the cfDNA NEPC Risk  
532 Score in men with mCRPC. Finally, the novel methods reported in this manuscript are an  
533 important step towards broadening the clinical applicability of blood-based epigenomic assays  
534 by providing a framework for non-invasive detection of tumor subtypes with distinct DNA  
535 methylation profiles.

536

537 **ACKNOWLEDGMENTS:** J. Berchuck is supported by the Department of Defense  
538 (W81XWH-20-1-0118). S. Baca is supported by a fellowship from the PhRMA Foundation and  
539 the Kure It Cancer Research Foundation. K. Korthauer is supported by the Natural Sciences and  
540 Engineering Research Council of Canada. Establishment and characterization of the LuCaP PDX  
541 models has been supported by the Pacific Northwest Prostate Cancer SPORE (P50CA97186), the



542 Department of Defense Prostate Cancer Biorepository Network (W81XWH-14-2-0183), the  
543 National Cancer Institute P01 CA163227, the Prostate Cancer Foundation, the Institute for  
544 Prostate Cancer Research, and the Richard M. Lucas Foundation. M. Pomerantz, H. Beltran, and  
545 M. Freedman are supported by a DFCI Medical Oncology grant award. H. Beltran is supported  
546 by the National Cancer Institute (5R37CA241486). M. Freedman is supported by the Claudia  
547 Adams Barr Program for Innovative Cancer Research, the H.L. Snyder Medical Research  
548 Foundation, and the Cutler Family Fund for Prevention and Early Detection.

549

## 550 **REFERENCES**

551

- 552 1. Aggarwal R, Huang J, Alumkal JJ, Zhang L, Feng FY, Thomas GV, et al. Clinical and  
553 Genomic Characterization of Treatment-Emergent Small-Cell Neuroendocrine Prostate  
554 Cancer: A Multi-institutional Prospective Study. *J Clin Oncol Off J Am Soc Clin Oncol.*  
555 2018;36:2492–503.
- 556 2. Abida W, Cyrta J, Heller G, Prandi D, Armenia J, Coleman I, et al. Genomic correlates of  
557 clinical outcome in advanced prostate cancer. *Proc Natl Acad Sci U S A.* 2019;116:11428–  
558 36.
- 559 3. Abida W, Cyrta J, Heller G, Prandi D, Armenia J, Coleman I, et al. Genomic correlates of  
560 clinical outcome in advanced prostate cancer. *Proc Natl Acad Sci. National Academy of*  
561 *Sciences;* 2019;116:11428–36.

- 562 4. Humeniuk MS, Gupta RT, Healy P, McNamara M, Ramalingam S, Harrison M, et al.  
563 Platinum sensitivity in metastatic prostate cancer: does histology matter? *Prostate Cancer*  
564 *Prostatic Dis.* 2018;21:92–9.
- 565 5. Beltran H, Prandi D, Mosquera JM, Benelli M, Puca L, Cyrta J, et al. Divergent clonal  
566 evolution of castration-resistant neuroendocrine prostate cancer. *Nat Med.* 2016;22:298–  
567 305.
- 568 6. Gundem G, Van Loo P, Kremeyer B, Alexandrov LB, Tubio JMC, Papaemmanuil E, et al.  
569 The evolutionary history of lethal metastatic prostate cancer. *Nature.* 2015;520:353–7.
- 570 7. Beltran H, Romanel A, Conteduca V, Casiraghi N, Sigouros M, Franceschini GM, et al.  
571 Circulating tumor DNA profile recognizes transformation to castration-resistant  
572 neuroendocrine prostate cancer. *J Clin Invest.* 2020;130:1653–68.
- 573 8. Shen SY, Singhania R, Fehringer G, Chakravarthy A, Roehrl MHA, Chadwick D, et al.  
574 Sensitive tumour detection and classification using plasma cell-free DNA methylomes.  
575 *Nature.* 2018;563:579–83.
- 576 9. Shen SY, Burgener JM, Bratman SV, De Carvalho DD. Preparation of cfMeDIP-seq libraries  
577 for methylome profiling of plasma cell-free DNA. *Nat Protoc.* 2019;14:2749–80.
- 578 10. Nuzzo PV, Berchuck JE, Korthauer K, Spisak S, Nassar AH, Abou Alaiwi S, et al. Detection  
579 of renal cell carcinoma using plasma and urine cell-free DNA methylomes. *Nat Med.*  
580 2020;26:1041–3.

- 581 11. Epstein JI, Amin MB, Beltran H, Lotan TL, Mosquera J-M, Reuter VE, et al. Proposed  
582 morphologic classification of prostate cancer with neuroendocrine differentiation. *Am J*  
583 *Surg Pathol.* 2014;38:756–67.
- 584 12. Nguyen HM, Vessella RL, Morrissey C, Brown LG, Coleman IM, Higano CS, et al. LuCaP  
585 Prostate Cancer Patient-Derived Xenografts Reflect the Molecular Heterogeneity of  
586 Advanced Disease and Serve as Models for Evaluating Cancer Therapeutics. *The*  
587 *Prostate.* 2017;77:654–71.
- 588 13. Adalsteinsson VA, Ha G, Freeman SS, Choudhury AD, Stover DG, Parsons HA, et al.  
589 Scalable whole-exome sequencing of cell-free DNA reveals high concordance with  
590 metastatic tumors. *Nat Commun.* 2017;8:1324.
- 591 14. Ewels P, Magnusson M, Lundin S, Källner M. MultiQC: summarize analysis results for  
592 multiple tools and samples in a single report. *Bioinforma Oxf Engl.* 2016;32:3047–8.
- 593 15. Langmead B, Salzberg SL. Fast gapped-read alignment with Bowtie 2. *Nat Methods.*  
594 2012;9:357–9.
- 595 16. Li H, Handsaker B, Wysoker A, Fennell T, Ruan J, Homer N, et al. The Sequence  
596 Alignment/Map format and SAMtools. *Bioinforma Oxf Engl.* 2009;25:2078–9.
- 597 17. Lienhard M, Grimm C, Morkel M, Herwig R, Chavez L. MEDIPS: genome-wide differential  
598 coverage analysis of sequencing data derived from DNA enrichment experiments.  
599 *Bioinforma Oxf Engl.* 2014;30:284–6.

- 600 18. Law CW, Chen Y, Shi W, Smyth GK. voom: Precision weights unlock linear model analysis  
601 tools for RNA-seq read counts. *Genome Biol.* 2014;15:R29.
- 602 19. Robinson MD, Oshlack A. A scaling normalization method for differential expression  
603 analysis of RNA-seq data. *Genome Biol.* 2010;11:R25.
- 604 20. Cavalcante RG, Sartor MA. annotatr: genomic regions in context. *Bioinformatics. Oxford*  
605 *Academic;* 2017;33:2381–3.
- 606 21. Amemiya HM, Kundaje A, Boyle AP. The ENCODE Blacklist: Identification of Problematic  
607 Regions of the Genome. *Sci Rep.* 2019;9:9354.
- 608 22. Zhang Y, Liu T, Meyer CA, Eeckhoute J, Johnson DS, Bernstein BE, et al. Model-based  
609 analysis of ChIP-Seq (MACS). *Genome Biol.* 2008;9:R137.
- 610 23. Pelizzola M, Koga Y, Urban AE, Krauthammer M, Weissman S, Halaban R, et al. MEDME:  
611 an experimental and analytical methodology for the estimation of DNA methylation levels  
612 based on microarray derived MeDIP-enrichment. *Genome Res.* 2008;18:1652–9.
- 613 24. Cejas P, Xie Y, Font-Tello A, Lim K, Syamala S, Qiu X, et al. Subtype heterogeneity and  
614 epigenetic convergence in neuroendocrine prostate cancer. *Nat Commun.* 2021;12:5775.
- 615 25. Dong B, Miao J, Wang Y, Luo W, Ji Z, Lai H, et al. Single-cell analysis supports a luminal-  
616 neuroendocrine transdifferentiation in human prostate cancer. *Commun Biol.* 2020;3:778.
- 617 26. McLean CY, Bristor D, Hiller M, Clarke SL, Schaar BT, Lowe CB, et al. GREAT improves  
618 functional interpretation of cis-regulatory regions. *Nat Biotechnol.* 2010;28:495–501.

- 619 27. Mayrhofer M, De Laere B, Whittington T, Van Oyen P, Ghysel C, Ampe J, et al. Cell-free  
620 DNA profiling of metastatic prostate cancer reveals microsatellite instability, structural  
621 rearrangements and clonal hematopoiesis. *Genome Med.* 2018;10:85.
- 622 28. Wu A, Cremaschi P, Wetterskog D, Conteduca V, Franceschini GM, Kleftogiannis D, et al.  
623 Genome-wide plasma DNA methylation features of metastatic prostate cancer. *J Clin*  
624 *Invest. American Society for Clinical Investigation*; 2020;130:1991–2000.
- 625 29. Wyatt AW, Annala M, Aggarwal R, Beja K, Feng F, Youngren J, et al. Concordance of  
626 Circulating Tumor DNA and Matched Metastatic Tissue Biopsy in Prostate Cancer. *JNCI J*  
627 *Natl Cancer Inst [Internet]*. 2017 [cited 2019 Aug 11];109. Available from:  
628 <https://www.ncbi.nlm.nih.gov/pmc/articles/PMC6440274/>
- 629 30. NCCN Clinical Practice Guidelines in Oncology: Prostate Cancer (Version 1.2022)  
630 [Internet]. 2021. Available from:  
631 [https://www.nccn.org/professionals/physician\\_gls/pdf/prostate.pdf](https://www.nccn.org/professionals/physician_gls/pdf/prostate.pdf)
- 632 31. Berchuck JE, Viscuse PV, Beltran H, Aparicio A. Clinical considerations for the  
633 management of androgen indifferent prostate cancer. *Prostate Cancer Prostatic Dis.* 2021;
- 634 32. Lasseter K, Nassar AH, Hamieh L, Berchuck JE, Nuzzo PV, Korthauer K, et al. Plasma cell-  
635 free DNA variant analysis compared with methylated DNA analysis in renal cell  
636 carcinoma. *Genet Med Off J Am Coll Med Genet.* 2020;22:1366–73.
- 637 33. Parikh AR, Seventer EEV, Siravegna G, Hartwig AV, Jaimovich A, He Y, et al. Minimal  
638 Residual Disease Detection using a Plasma-Only Circulating Tumor DNA Assay in  
639 Colorectal Cancer Patients. *Clin Cancer Res [Internet]*. American Association for Cancer

- 640 Research; 2021 [cited 2021 May 5]; Available from:  
641 <https://clincancerres.aacrjournals.org/content/early/2021/04/28/1078-0432.CCR-21-0410>
- 642 34. Liu MC, Oxnard GR, Klein EA, Swanton C, Seiden MV, Liu MC, et al. Sensitive and  
643 specific multi-cancer detection and localization using methylation signatures in cell-free  
644 DNA. *Ann Oncol.* Elsevier; 2020;31:745–59.
- 645 35. Saghafeinia S, Mina M, Riggi N, Hanahan D, Ciriello G. Pan-Cancer Landscape of Aberrant  
646 DNA Methylation across Human Tumors. *Cell Rep.* 2018;25:1066-1080.e8.
- 647 36. Noushmehr H, Weisenberger DJ, Diefes K, Phillips HS, Pujara K, Berman BP, et al.  
648 Identification of a CpG island methylator phenotype that defines a distinct subgroup of  
649 glioma. *Cancer Cell.* 2010;17:510–22.
- 650 37. Cancer Genome Atlas Network. Comprehensive molecular characterization of human colon  
651 and rectal cancer. *Nature.* 2012;487:330–7.
- 652 38. Cancer Genome Atlas Research Network, Kandoth C, Schultz N, Cherniack AD, Akbani R,  
653 Liu Y, et al. Integrated genomic characterization of endometrial carcinoma. *Nature.*  
654 2013;497:67–73.
- 655  
656

657 **TABLES**

658

659 **Table 1.** Patient characteristics at the time of cfDNA collection in the test and validation cohorts  
 660 of men with mCRPC.

661

	Test Cohort		Validation Cohort	
	NEPC N = 9	PRAD N = 39	NEPC N = 12	PRAD N = 41
<b>Median cfDNA Tumor Content (Range)</b>	15% (5.1-75%)	21% (3.3-80%)	23% (3.4-43%)	16% (3.8-49%)
<b>Median Age (Range)</b>	72 (60-84)	71 (61-92)	71 (54-91)	70 (49-86)
<b>Median PSA (Range)</b>	0.37 (0.03-3.7)	140 (0.79-4305)	0.33 (0.01-6.23)	112 (4.5-1821)
<b><i>De Novo</i> NEPC</b>	3 (33%)	N/A	2 (17%)	N/A
<b>Prior Local Therapy</b>	5 (56%)	27 (69%)	5 (42%)	26 (63%)
<b>Prior ADT</b>	4 (44%)	39 (100%)	8 (67%)	41 (100%)
<b>Prior Abiraterone or Enzalutamide</b>	0 (0%)	36 (92%)	4 (33%)	39 (95%)
<b>Prior Docetaxel</b>	2 (22%)	25 (64%)	2 (17%)	35 (85%)
<b>Prior EP Chemotherapy</b>	7 (78%)	0 (0%)	8 (67%)	0 (0%)
<b>Liver Metastases</b>	3 (33%)	15 (38%)	8 (67%)	13 (32%)

662

663 Abbreviations: mCRPC, metastatic castration-resistant prostate cancer; cfDNA, cell-free DNA;  
 664 NEPC, neuroendocrine prostate cancer; PRAD, prostate adenocarcinoma; PSA, prostate-specific  
 665 antigen; N/A, not applicable; ADT, androgen deprivation therapy; ARSI, androgen receptor  
 666 signaling inhibitor; EP, etoposide plus platinum.

667

668 **FIGURE LEGENDS**

669

670 **Figure 1.** Identification of tumor-derived PRAD-enriched and NEPC-enriched DMRs. **A)**

671 Overview of the methods used to detect the presence of NEPC based on tissue-informed cfDNA

672 analysis. **B)** Volcano plot showing differentially methylated regions (DMRs) between PRAD

673 (N=24) and NEPC (N=5) patient-derived xenografts. Red and blue dots represent NEPC-

674 enriched PRAD-enriched (N=137,692) and NEPC-enriched (N=39,699) DMRs, respectively,

675 with FDR-adjusted  $P < 0.05$ . **C)** Correlation between tumor-derived DMRs with differentially

676 methylated nucleotides in reduced representation bisulfite sequencing (RRBS) data from CR-

677 PRAD and NEPC tumors.(5) **D)** Tracks depict methylation at the *SPDEF* gene and *UNC13A*

678 gene determined by MeDIP-seq in PRAD tumors, NEPC tumors, and white blood cells (WBCs).

679 **E)** The top 5 gene ontology (GO) enrichment terms for PRAD-enriched and NEPC-enriched

680 DMRs after removing sites with DNA methylation in WBCs.

681

682 **Figure 2.** Classification of NEPC and PRAD samples in the cfDNA test cohort. NEPC

683 Methylation Values (**A**), PRAD Methylation Values (**B**), and NEPC Risk Scores (**C**) in cfDNA

684 samples from men with PRAD or NEPC in the test cohort. P-Values calculated using a two-sided

685 Wilcoxon rank-sum test. Optimal cut-off (indicated by dotted gray line) was determined in this

686 cohort using Youden's J statistic. **D)** Kaplan-Meier curve for overall survival (OS) from the time

687 of metastatic disease for men with high ( $>0.15$ ) versus low ( $\leq 0.15$ ) NEPC Risk Score relative to

688 the cut-off.

689



690 **Figure 3.** Classification of NEPC and PRAD samples in the cfDNA validation cohort. NEPC  
691 Methylation Values (**A**), PRAD Methylation Values (**B**), and NEPC Risk Scores (**C**) in cfDNA  
692 samples from men with NEPC or PRAD in the validation cohort. P-Values calculated using a  
693 two-sided Wilcoxon rank-sum test. The optimal NEPC Risk Score cut-off determined in the  
694 independent cfDNA test cohort is indicated by dotted gray line. **D**) Kaplan-Meier curve for  
695 overall survival (OS) from the time of metastatic disease for men with high ( $>0.15$ ) versus low  
696 ( $\leq 0.15$ ) NEPC Risk Score relative to the cut-off determined in the independent cfDNA test  
697 cohort.

698

699 **Figure 4.** cfDNA from men with CR-PRAD with high NEPC Risk Scores display clinical and  
700 genomic features of NEPC.

701

702 **Figure 5.** Association of the plasma cfDNA methylome with NEPC Risk Score and tumor  
703 content. **A**) Principal component analysis (PCA) of the genome-wide methylome for 101 plasma  
704 cfDNA samples from men with CR-PRAD or NEPC. **B**) PCA of the 101 plasma cfDNA samples  
705 limiting to the NEPC- and PRAD-enriched DMRs included in the NEPC Risk Score. Correlation  
706 between NEPC Risk Score with the top 10 principal components (PCs) for the cfDNA genome-  
707 wide methylome data (**C**) and restricted to the DMR sites (**D**). Correlation between cfDNA  
708 tumor content with the top 10 PCs for the cfDNA genome-wide methylome data (**E**) and  
709 restricted to the DMR sites (**F**). Correlation between NEPC Risk Score and each PC was  
710 measured using the coefficient of determination ( $R^2$ ). \*  $P < 0.05$ ; \*\*  $P < 1 \times 10^{-6}$ . **G**) Correlation  
711 between NEPC Risk Score and tumor content for the 101 cfDNA samples from men with NEPC

712 and CR-PRAD. Dotted lines show the linear regression for the NEPC samples (red), CR-PRAD  
713 samples (blue), and all samples (purple).

**Figure 1**

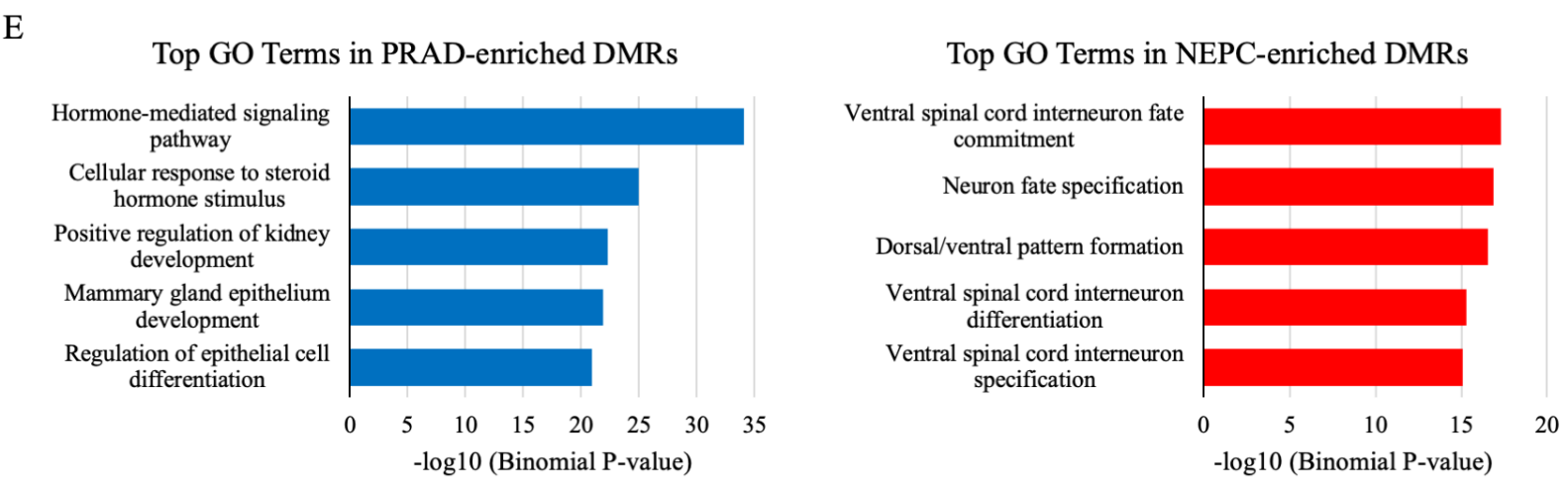
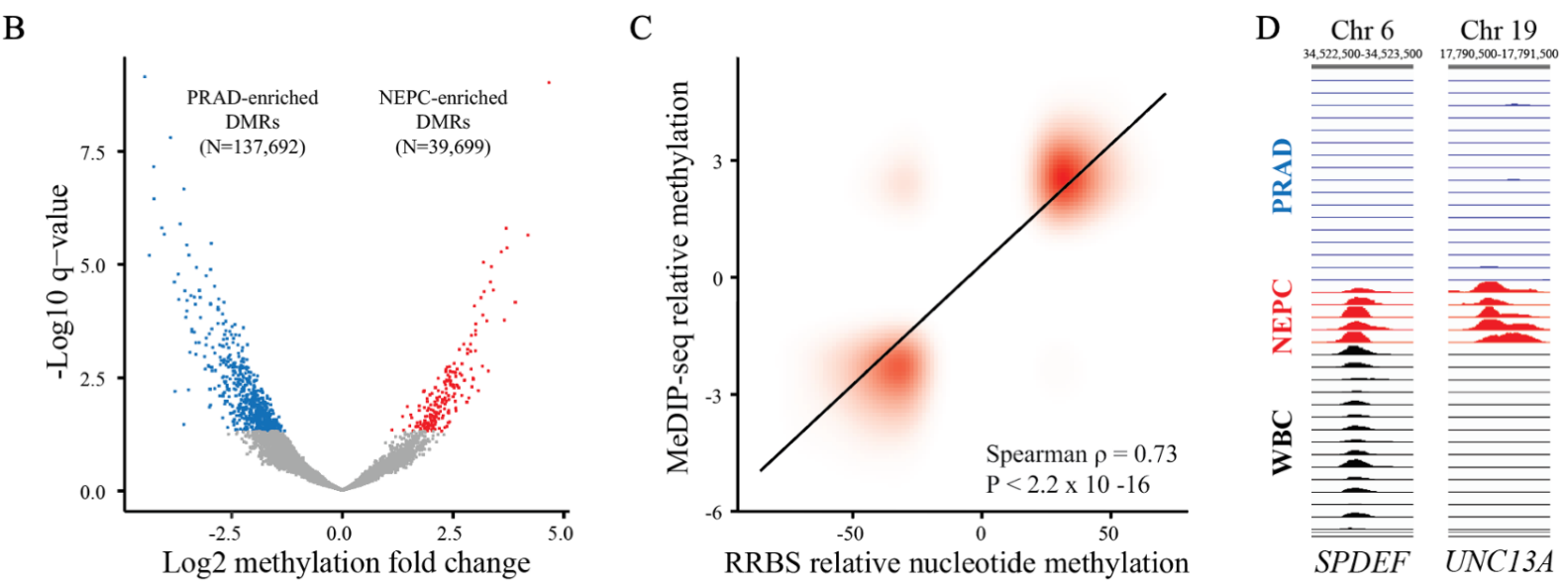
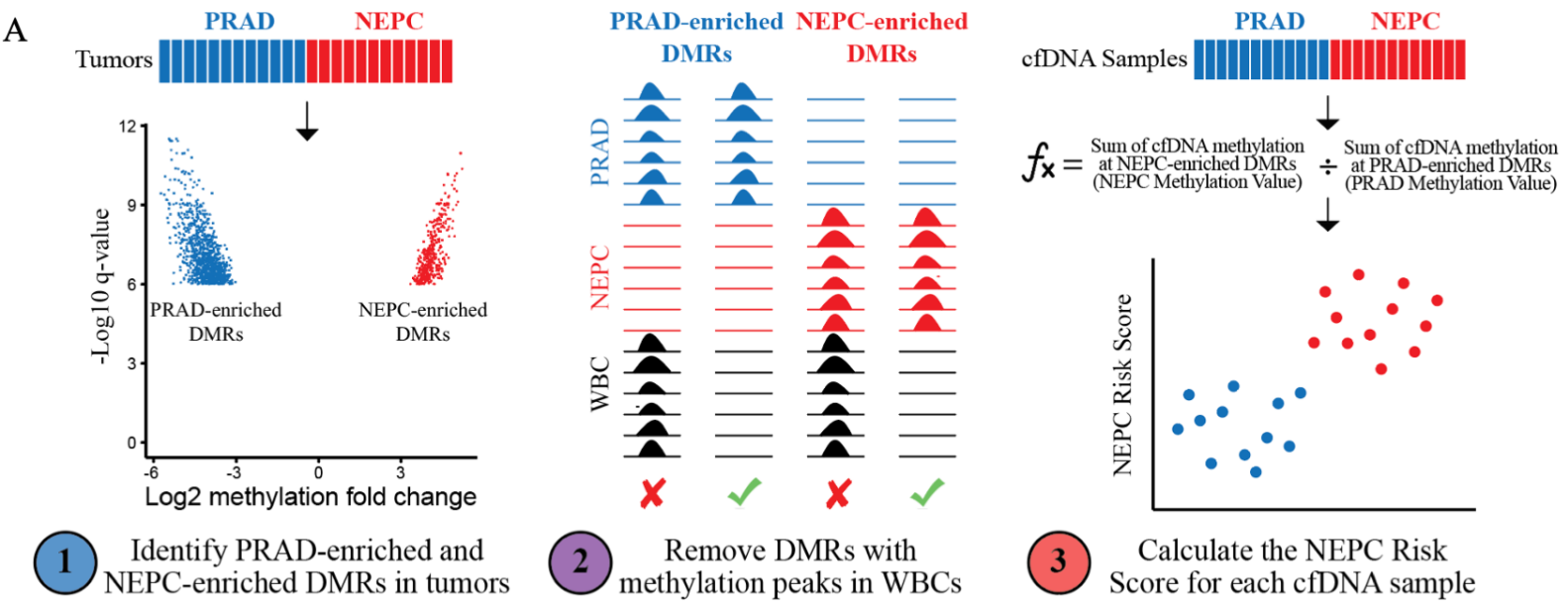


# Figure 2

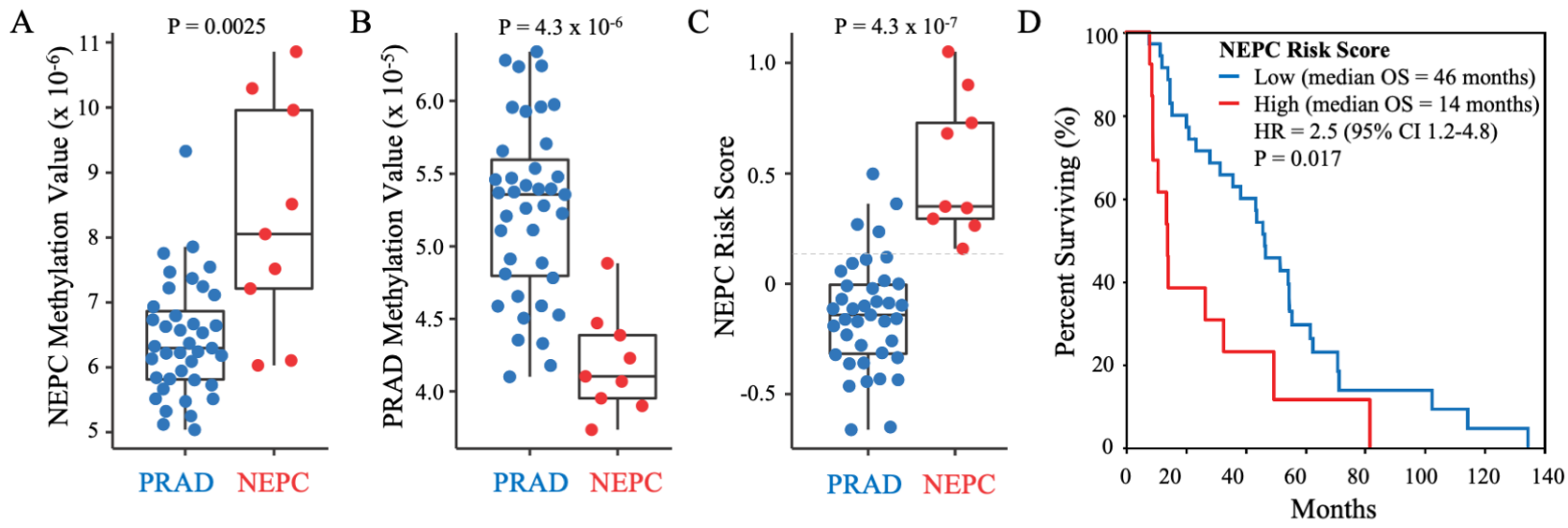


### Figure 3

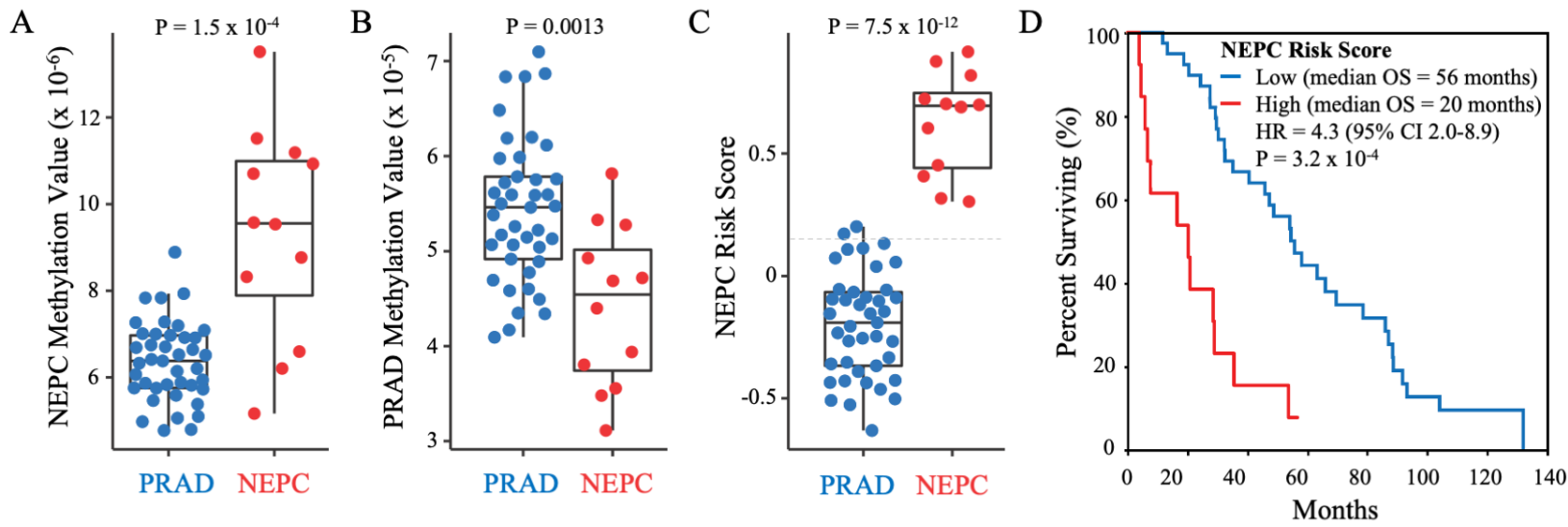
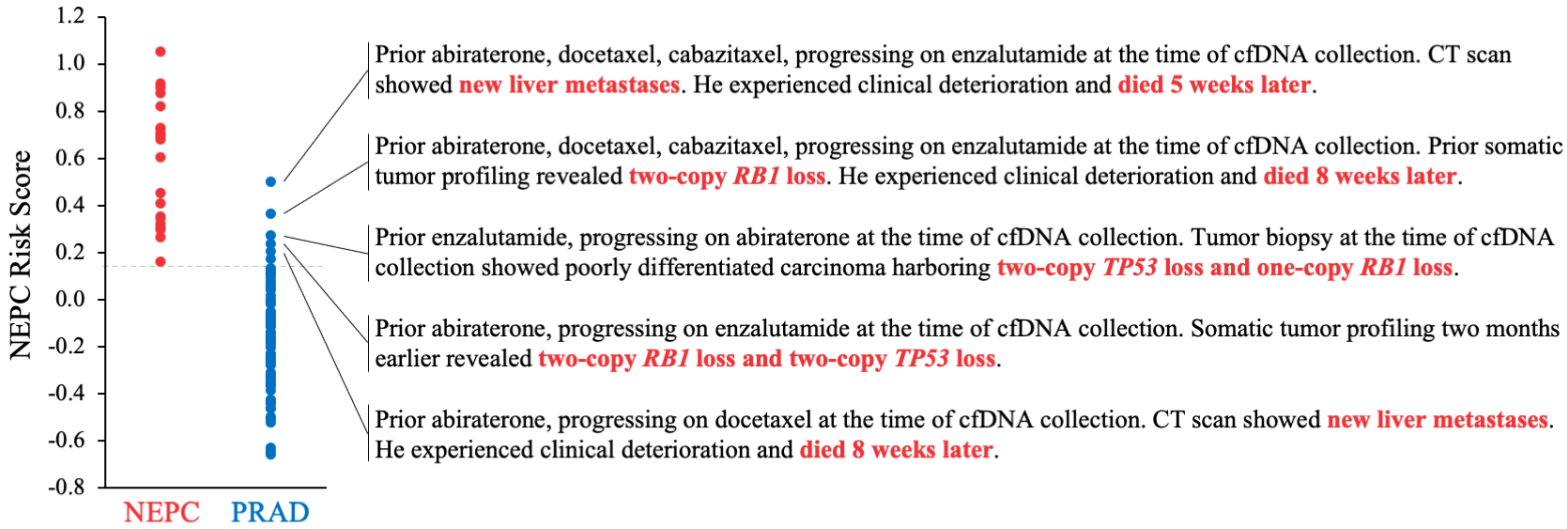
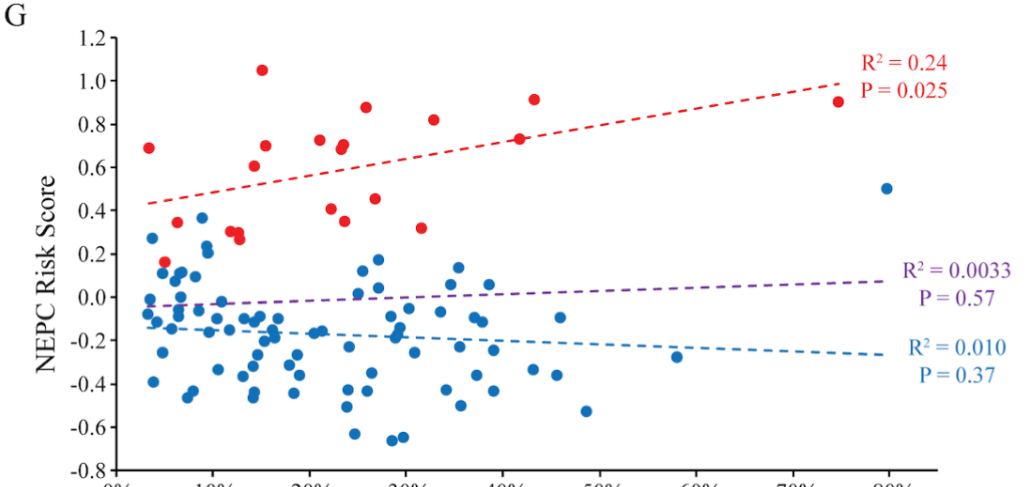
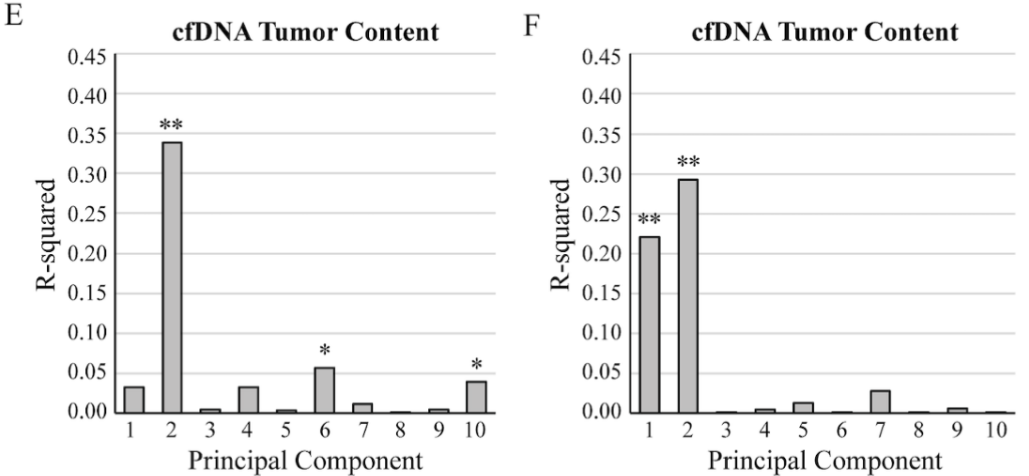
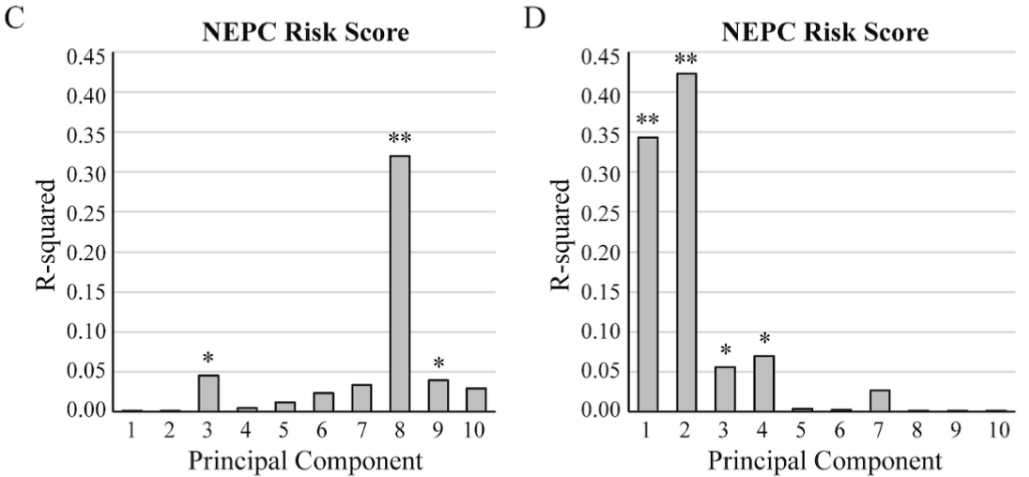
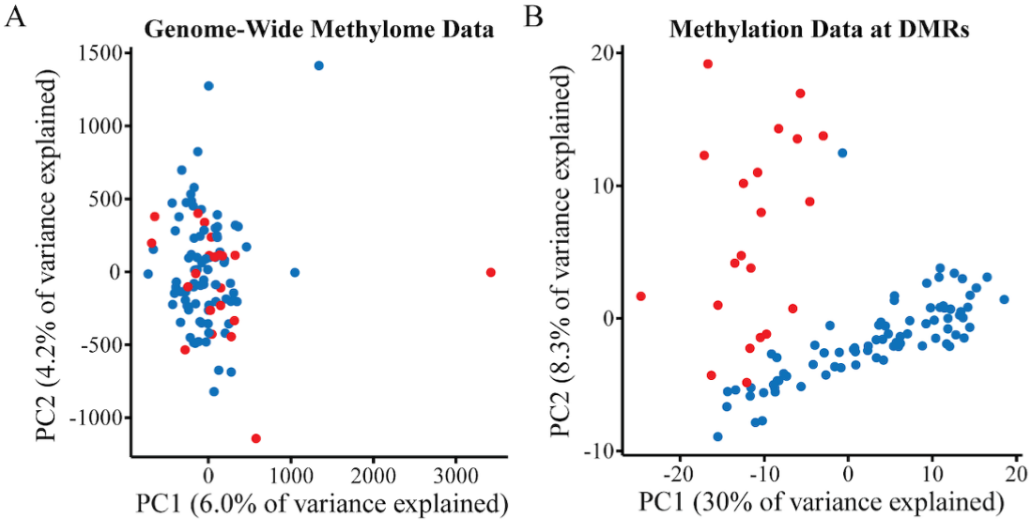


Figure 4



# Figure 5



# Clinical Cancer Research

## Detecting neuroendocrine prostate cancer through tissue-informed cell-free DNA methylation analysis

Jacob E. Berchuck, Sylvan C. Baca, Heather M. McClure, et al.

*Clin Cancer Res* Published OnlineFirst December 14, 2021.

<b>Updated version</b>	Access the most recent version of this article at: doi: <a href="https://doi.org/10.1158/1078-0432.CCR-21-3762">10.1158/1078-0432.CCR-21-3762</a>
<b>Supplementary Material</b>	Access the most recent supplemental material at: <a href="http://clincancerres.aacrjournals.org/content/suppl/2021/12/14/1078-0432.CCR-21-3762.DC1">http://clincancerres.aacrjournals.org/content/suppl/2021/12/14/1078-0432.CCR-21-3762.DC1</a>
<b>Author Manuscript</b>	Author manuscripts have been peer reviewed and accepted for publication but have not yet been edited.

**E-mail alerts** [Sign up to receive free email-alerts](#) related to this article or journal.

**Reprints and Subscriptions** To order reprints of this article or to subscribe to the journal, contact the AACR Publications Department at [pubs@aacr.org](mailto:pubs@aacr.org).

**Permissions** To request permission to re-use all or part of this article, use this link <http://clincancerres.aacrjournals.org/content/early/2021/12/13/1078-0432.CCR-21-3762>. Click on "Request Permissions" which will take you to the Copyright Clearance Center's (CCC) Rightslink site.